Received: 8 March 2023 | Accepted: 8 July 2023

DOI: 10.1111/1751-7915.14321

MICROBIAL BIOTECHNOLOGY Applied Microbiology International

RESEARCH ARTICLE

Steerable isobutyric and butyric acid production from CO_2 and H_2 by *Clostridium luticellarii*

Quinten Mariën[1,2] | **Alberte Regueira**[1,2,3] | **Ramon Ganigué**[1,2]

[1]Center for Microbial Ecology and Technology (CMET), Ghent University, Ghent, Belgium

[2]Center for Advanced Process Technology for Urban Resource Recovery (CAPTURE), Ghent, Belgium

[3]CRETUS, Department of Chemical Engineering, Universidade de Santiago de Compostela, Santiago de Compostela, Spain

Correspondence
Ramon Ganigué, Center for Microbial Ecology and Technology (CMET), Faculty of Bioscience Engineering, Ghent University, Coupure Links 653, B-9000 Ghent, Belgium.
Email: ramon.ganigue@ugent.be

Funding information
Galician Competitive Research Group, Grant/Award Number: ERDF (UE) and GRC ED431C 2021/37; Bijzonder Onderzoeksfonds UGent, Grant/Award Number: BOF19/STA/044; Fonds Wetenschappelijk Onderzoek, Grant/Award Number: 1SC5722N; Xunta de Galicia, Grant/Award Number: ED481B-2021-012

Abstract

Clostridium luticellarii is a recently discovered acetogen that is uniquely capable of producing butyric and isobutyric acid from various substrates (e.g. methanol), but it is unclear which factors influence its (iso)butyric acid production from H_2 and CO_2. We aimed to investigate the autotrophic metabolism of *C. luticellarii* by identifying the necessary growth conditions and examining the effects of pH and metabolite levels on product titers and selectivity. Results show that autotrophic growth of *C. luticellarii* requires the addition of complex nutrient sources and the absence of shaking conditions. Further experiments combined with thermodynamic calculations identified pH as a key parameter governing the direction of metabolic fluxes. At circumneutral pH (~6.5), acetic acid is the sole metabolic end product but *C. luticellarii* possesses the unique ability to co-oxidize organic acids such as valeric acid under high H_2 partial pressures (>1 bar). Conversely, mildly acidic pH (≤5.5) stimulates the production of butyric and isobutyric acid while partly halting the oxidation of organic acids. Additionally, elevated acetic acid concentrations stimulated butyric and isobutyric acid production up to a combined selectivity of 53 ± 3%. Finally, our results suggest that isobutyric acid is produced by a reversible isomerization of butyric acid, but valeric and caproic acid are not isomerized. These combined insights can inform future efforts to optimize and scale-up the production of valuable chemicals from CO_2 using *C. luticellarii*.

BACKGROUND

Since the onset of the industrial revolution, atmospheric carbon dioxide (CO_2) concentrations have been increasing at a rapid pace due to anthropogenic activities (Song, 2006). Global emissions of greenhouse gases amounted to 36 Gtons of CO_2 equivalents per year in 2020 (Ritchie 2021), of which approximately 29% resulted from a limited number of energy-intensive industries (the most notorious being the steel and iron, cement, (petro)chemical and paper and pulp industries) (Koytsoumpa et al., 2018; European Commission, Joint Research Centre, 2021). These industries form interesting targets for the carbon capture and utilization (CCU) concept, in which CO_2 is captured at the point of emission or after emission and used as a feedstock for the production of added-value compounds such as platform chemicals (e.g. methanol or organic acids), plastics or biofuels (Boot-Handford et al., 2014; Martens et al., 2017). CCU thereby decreases both direct CO_2 emissions and the dependence of the chemical industry on fossil fuels as carbon source (Garcia-Garcia et al., 2021).

One interesting technology for CCU, gas fermentation, harnesses acetogens, a group of strict anaerobic bacteria. Acetogens are highly flexible microorganisms: they can grow on a wide variety of organic compounds such as carbohydrates and methylated

compounds such as methylamines, methanol or formic acid (Drake, 1995; Schuchmann & Müller, 2014). The most fascinating part of their metabolism, however, lies in their facultative autotrophic behaviour, meaning that they can grow on inorganic carbon sources such as CO_2 using inorganic electron sources such as H_2 and CO (Schuchmann & Müller, 2014). Their carbon-fixating pathway, the Wood-Ljungdahl Pathway (WLP), is considered one of the most energy-efficient carbon fixating pathways in nature, achieving energetic efficiencies of 55%–95% depending on the C1 carbon source, rendering acetogens interesting biocatalysts for CCU (Claassens et al., 2019).

In the WLP, two CO_2 molecules are reduced with electrons coming from, for example, H_2 oxidation to, respectively, a methyl and carbonyl group, which are condensed together with coenzyme A (CoA) to the central intermediate acetyl-CoA (Schuchmann & Müller, 2014). While most acetogens rely on converting that acetyl-CoA to acetic acid as the sole possible end-product of their metabolism, several can produce more valuable end-metabolites (Bengelsdorf et al., 2018). For example, the acetogen *Clostridium autoethanogenum* is currently used at a commercial scale by Lanzatech to convert carbonaceous off-gases from steel mills (mainly CO) to ethanol (Liew et al., 2016). However, the production of longer-chain products is gaining increased interest due to their substantially higher market value (e.g. butyric acid has 3–5 times higher value than acetic acid) (Calvo et al., 2022; Kim et al., 2019). Several acetogens have been shown to convert CO_2, CO and/or organic C1 compounds to these longer acids via a process called chain elongation. This process uses the reverse β-oxidation pathway where two acetyl-CoA molecules (either produced via the WLP or assimilated from acetic acid) are condensed to acetoacetyl-CoA which is subsequently transformed and reduced (with electrons coming from H_2 oxidation) to butyryl-CoA and finally converted to butyric acid. As such, the carbon chain of acetyl-CoA (or acetic acid) is elongated with two carbon atoms to butyric acid, which in some acetogens can be elongated in a second chain elongation cycle to caproic acid (Bengelsdorf et al., 2018). Examples of chain elongating acetogens include: *Eubacterium limosum*, able to produce acetic and butyric acid from C1 compounds (Litty & Müller, 2021); *Butyribacterium methylotrophicum*, capable of producing the same products and also their respective alcohols, ethanol and butanol (Worden et al., 1991); and *C. carboxidivorans*, able to produce acetic acid, butyric acid, caproic acid and their respective alcohols (Ramió-Pujol et al., 2015).

Nevertheless, while many acetogens have these interesting metabolic properties and end-products, they do not produce significant amounts of products beyond acetic acid autotrophically at optimal growth conditions (Litty & Müller, 2021; Richter et al., 2016). However, suboptimal growth conditions such as low pH have been reported to stimulate shifts in product spectrum from organic acids to alcohol production (Abubackar et al., 2012; Arslan et al., 2019; Fernández-Naveira et al., 2016; Martin et al., 2016), and from acetic acid and ethanol to butyric acid and butanol (Worden et al., 1991). Similarly, high concentrations of intermediate metabolic products (i.e. acetic acid) have been reported to stimulate chain elongation from methanol and CO_2 in methylotrophic acetogens (Lynd & Zeikus, 1983; Pacaud et al., 1986; Petrognani et al., 2020), although this effect seems to be less studied under autotrophic growth conditions.

The recently isolated acetogen *Clostridium luticellarii* was found to produce butyric and isobutyric acid from methanol and CO_2, hypothetically via the WLP and consecutive reverse β-oxidation to butyric acid and isobutyric acid (Petrognani et al., 2020; Wang et al., 2015). Both butyric and isobutyric acids are interesting platform molecules. The former has applications in food additives, fragrances, antibacterial agents and bioplastics, while its branched isomer has a high market volume as a precursor for poly-methyl methacrylate (acrylic glass) with a market size of 2.7 million tons per year (Lang et al., 2014; Moscoviz et al., 2018). Since both the compounds are currently produced from petrochemically derived propylene (Zhang et al., 2011), establishing a direct route to biologically produce butyric and isobutyric acid from CO_2 and H_2 could greatly improve their sustainability as high-volume platform chemicals while simultaneously capturing carbon. However, it currently remains unclear whether *C. luticellarii* is able to grow autotrophically and which factors influence its (iso)butyric acid production from H_2 and CO_2. Here, we elucidate the autotrophic growth capacity of *C. luticellarii* and how its butyric and isobutyric acid production is affected by the presence of increased concentrations of intermediate and end-products. Next, the impact of pH as a factor governing the production of longer-chain products was investigated. Finally, a thermodynamic approach was used to understand the metabolic flexibility of *C. luticellarii* under diverse environmental conditions.

EXPERIMENTAL PROCEDURES

Inoculum and media preparation

Clostridium luticellarii DSM 29923 was obtained from the German Collection of Microorganisms and Cell Cultures (DSMZ, Braunschweig, Germany). The strain was activated at pH 7.2 and 37°C on Reinforced Clostridial medium (RCM, as described by Petrognani et al. (2020)) and sub-cultured at pH 6.5 on basal medium (10% v/v inoculum ratio) with 200 mM methanol and 40 mM $NaHCO_3$ as carbon sources before transferring to autotrophic growth conditions on basal medium. An inoculum ratio of 10% (v/v%) was used in all experiments

unless stated otherwise. Non-inoculated controls were used alongside each subculture and experimental run to check for contaminations and the purity of the culture was regularly checked via microscopic examination and Sanger sequencing of the 16S rRNA gene.

The basal medium contained (per 1 L): 0.36 g $NH_4H_2PO_4$; 0.133 g $CaCl_2$; 0.325 g $MgCl_2.6H_2O$; 0.197 g $MgSO_4.7H_2O$; 0.149 KCl; 14.643 g 2-(N-morpholino) ethanesulfonic acid (MES) buffer; and 0.001 g resazurine. The basal medium was boiled, cooled down under continuous sparging of N_2 and dispensed in 1 L Duran pressure plus Schott bottles under an N_2 atmosphere. Subsequently, the headspace of the bottles was flushed with N_2 for at least 15 min. After autoclaving, the headspace of the bottles was flushed with filter sterilized H_2/CO_2 (80/20 v/v%) for at least 15 min and pressurized to 150 kPa absolute. Before inoculation, vitamins and trace elements (Tables S1–S3), 30 mM $NaHCO_3$, 0.4 mM titanium (III) citrate (reducing agent) and 0.5 g L^{-1} tryptone (only added in the experiments detailed in Impact of organic acid addition and pH on the autotrophic metabolism) were added to the basal medium from anaerobic filter sterilized concentrated stock solutions.

Batch experiments

Impact of environmental and operational conditions enabling autotrophic growth

Experiments were conducted using various media compositions to pinpoint the conditions enabling the autotrophic growth of *C. luticellarii*. First, four conditions were tested in triplicate in 1050 mL bottles (Duran Pressure Plus) with 75 mL working volume: (i) growth on basal medium without the addition of any complex nutrient sources, (ii) growth on basal medium with twice concentrated vitamins and trace elements, (iii) addition of 1 g L^{-1} of yeast extract to (i), and (iv) addition of 0.5 g L^{-1} tryptone to (i). To eliminate any traces of methanol for the subsequent autotrophic experiments from the basal medium, the methylotrophic culture was sub-cultured once on a new basal medium containing no organic carbon sources under 150 kPa of an 80:20 H_2:CO_2 atmosphere and used as inoculum for the subsequent experiments. After the addition of the respective nutrient sources and adjustment of the pH to 6.5, the bottles were inoculated and incubated statically and horizontally (to maximize gas–liquid mass transfer area) at 37°C. Right after inoculation, and at regular time intervals, the headspace pressure was measured with a tensiometer (GMH 3111 equipped with a 603310 MSD 2.5 BAE sensor, Greisinger) and needle, gas samples (≈5.0 mL) were taken for immediate GC analysis and liquid samples (1.0 mL) were taken for immediate pH and OD measurements. The remaining liquid samples were filtered (0.20 μm) and stored at −18°C until HPLC analysis.

The impact of shaking incubation was investigated by comparing the growth of *C. luticellarii* incubated statically and horizontally, with incubation horizontally on a shaker at 150 rpm. Bottles were incubated at 37°C. The same medium as case (iv) described above was used. The pressure decrease was monitored daily by using a tensiometer with a needle as a proxy for gas consumption and growth. Experiments were conducted in triplicate in 250 mL penicillin bottles with 40 mL working volume to be able to rapidly and accurately detect the pressure decrease.

Impact of organic acid addition and pH on the autotrophic metabolism

The autotrophic product spectrum was characterized in further experiments using the medium described in Inoculum and media preparation with 0.5 g L^{-1} tryptone and by incubating bottles statically and horizontally (Table 1). To obtain a reference for comparison, *C. luticellarii* was grown in the first experiment under 150 kPa absolute of 80:20 H_2:CO_2 atmosphere and at pH 6.5. Simultaneously, the effect of organic acids addition at initial pH 6.5 was investigated by growing *C. luticellarii* in the presence of acetic acid (50 mM), butyric acid (50 mM), isobutyric acid (50 mM), valeric acid (25 mM) and caproic acid (25 mM). The next experiment further investigated the effect of valeric acid on autotrophic metabolism at initial pH 6.5 by growing *C. luticellarii* at different valeric acid concentrations of, respectively, 10 mM, 50 mM and 75 mM. A third experiment investigated the effect of pH by growing *C. luticellarii* at initial pH 5.5 and pH 6.5 while manually controlling the pH between 5.0–5.5 and 6.0–6.5, respectively. To that end, pH was measured on the taken samples, and 2 M NaOH was added to the bottles to correct the pH to 5.5 or 6.5 depending on the condition. This was done in three different scenarios: without organic acid addition, with acetic acid addition (50 mM) and with valeric acid addition (25 mM). All the conditions were tested in triplicate. A final fourth experiment was conducted in triplicate by incubating *C. luticellarii* with 25 mM valeric acid at pH 6.5 in the absence of H_2. The bottles were flushed with an N_2 and CO_2 gas mixture (N_2:CO_2 90:10) and pressurized to 150 kPa absolute.

After the addition of organic acids (except for conditions 1A, 3A and 3B), and adjustment of the pH, the bottles were inoculated with a 10% inoculum ratio (except for experiment 3 in which a 25% inoculum ratio was used for all conditions to minimize the lag phase in the conditions at pH 5.5) of *C. luticellarii* in end-exponential growth phase after at least sub-culturing two times on autotrophic growth medium. These experiments were carried out in Schott bottles of a total volume of 1050 mL with a 75 mL working volume, incubated statically, horizontally, and at 37°C. Sampling was carried out as described in Impact of environmental and operational conditions

TABLE 1 Summary of experimental conditions.

Experiment	Condition	Initial pH	Addition	Concentration (mM)	Inoculum ratio (% v/v)
1	A	6.5	–	–	10
	B		Acetic acid	50	
	C		Butyric acid	50	
	D		Isobutyric acid	50	
	E		Valeric acid	25	
	F		Caproic acid	25	
	G		Acetic acid	50	
			Butyric acid	50	
2	A	6.5	Valeric acid	10	10
	B			50	
	C			75	
3	A	6.5 (controlled)	–	–	25
	B	5.5 (controlled)	–	–	
	C	5.5 (controlled)	Acetic acid	50	
	D	6.5 (controlled)	Valeric acid	25	
	E	5.5 (controlled)	Valeric acid	25	
4	–	6.5	Valeric acid without H_2	25	10

enabling autotrophic growth. Experiments were sampled until no net decrease of headspace pressure was observed for two consecutive sampling moments.

Analytical methods

Carboxylic acids (C1, C2, C3, C4, C5, C6 including C4, C5 and C6 isoforms) and alcohols (ethanol, isobutanol, 1-butanol) were analysed by HPLC (LC-2030C Plus Prominence-© series, Shimadzu) equipped with an Aminex HPX-87H column (300 × 7.8 mm, BioRad) coupled with a Micro-Guard cartridge. Carboxylic acids and alcohols were quantified using a UV detector with wavelength 210 nm (UV/Vis SPD-40, Shimadzu) and a refractive index detector (RID-20A, Shimadzu), respectively. 20 μL of the sample was eluted with 5 mM H_2SO_4 and 1% acetonitrile at a flow rate of 0.45 mL min^{-1}. The column oven temperature was set at 30°C and the UV and RID cell temperatures were set at 40°C. The composition of the headspace was analysed using a Compact Gas Chromatograph (Global Analyser Solutions, Breda, The Netherlands), equipped with a Molsieve 5A pre-column and Porabond column (CH_4, O_2, H_2 and N_2) and an Rt-Q-bond pre-column and column (CO_2). Concentrations of gases were determined by means of a thermal conductivity detector. OD was measured on 250 μL aliquots at 620 nm in 96 well plates using a plate reader (Infinite M200 PRO, Tecan).

Calculations

Gas consumption

The absolute amount of gas *i* in the bottles was calculated from the measured headspace pressure and headspace composition of that gas using the ideal gas law according to equation 1:

$$n_i = \frac{PV}{RT}\chi_i \quad (1)$$

where n_i is the absolute amount of gas *i* (mol), *R* is the molar gas constant (8.31 J mol^{-1} K^{-1}), *T* is the temperature at which *P* was measured (310.15 K), *P* is the headspace pressure (Pa), χ_i is the molar fraction of gas *i* in the headspace and *V* is the headspace volume in the bottle (m^3).

The absolute amount of gas was calculated before and after every sampling point, using the change of headspace pressure in the control to determine the change in pressure due to sampling (~1 kPa per sample). The change between the absolute amount of gas after sampling on a certain timepoint and the gas amount before sampling on the next timepoint represented the gas consumption between two timepoints. These gas consumptions were summed over all timepoints to determine the total gas consumption (equation 2).

$$\text{total gas consumption of gas } i = \sum_{j=t_1}^{t_{end}} n_{i,j-1\ (\text{after sampling})} - n_{i,j\ (\text{before sampling})} \quad (2)$$

Metabolite production

The volumes taken during sampling were taken into account when calculating electron balances. The absolute amount of products was calculated before and after every sampling point by multiplication of the concentration with the volume in the bottles taking into account the change in liquid volume due to sampling. The change between the absolute amount of product after sampling on a certain timepoint and the absolute amount of product before sampling on the next timepoint represented the production between two timepoints. These productions were summed over all timepoints to determine the total production (equation 3).

$$\text{total production of compound } i = \sum_{j=t_1}^{t_{end}} m_{i,j\ (\text{before sampling})} - m_{i,j-1\ (\text{after sampling})} \quad (3)$$

where $m_{i,j}$ is the absolute amount of electron equivalents contained in compound i at time point j.

Carboxylic acid selectivity

The selectivity with which specific carboxylic acids were produced was calculated as the net absolute amount of electron equivalents (mol eeq.) of that specific carboxylic acid relative to the net electron equivalents of all produced carboxylic acids (equation 4).

$$\text{Carboxylic acid selectivity } (\%\text{el. eq.}) = \frac{\text{carboxylic acid (mol eeq.)}}{\sum \text{carboxylic acids (mol eeq.)}}\ 100\% \quad (4)$$

Thermodynamic calculations

The thermodynamics of the valeric acid oxidation pathway to propionic and acetic acid under an H_2-containing atmosphere were calculated in two cases: (i) oxidation of valeric acid assuming that protons are used as a final electron sink to produce H_2 (equation 5) and (ii) oxidation of valeric acid with using intracellular electron carriers as electron acceptors (equation 6), which are regenerated in other metabolic process such as the WLP.

$$C_5H_9O_2^- + 2\,H_2O \rightarrow C_3H_5O_2^- + C_2H_3O_2^- + H^+ + 2H_2 \quad (5)$$

$$C_5H_9O_2^- + 2\,Fd_{red} + 3\,NAD^+ + 2\,H_2O \rightarrow C_3H_5O_2^- + C_2H_3O_2^- + 2\,H^+ + 2\,Fd_{ox} + 3\,NADH \quad (6)$$

Electron confurcation (i.e. the reverse of electron bifurcation as occurring in valeric and butyric acid formation via reverse β-oxidation) was assumed in case (ii) for the oxidation of valeryl-CoA to pent-2-enoyl-CoA with NAD^+ where the oxidation needs an energy investment (provided by the exergonic NAD^+ reduction with ferredoxin) (González-Cabaleiro et al., 2013; Kleerebezem & Stams, 2000; Li et al., 2008).

Standard Gibbs free energy and enthalpy of formation of NADH were taken from Alberty (2003) and, in the case of Ferredoxin, the Gibbs free energy was calculated from the E°′ values (at standard conditions corrected for pH 7) described in the literature (~−450 mV (Battistuzzi et al., 2000; Bellei et al., 2010)) using the Nernst equation, while all other values were taken from Kleerebezem and Van Loosdrecht (2010). All used values are listed in Table S4. These values were used to calculate the standard Gibbs energy change of the reaction and the standard enthalpy change of reaction at 25°C and used to calculate the Gibbs energy change of reaction at 37°C for both cases as described by Kleerebezem and Van Loosdrecht (2010). The resulting Gibbs energy values (ΔG°′) were converted to account for realistic intracellular metabolite concentrations (i.e. 10 mM valeric acid and 1 mM propionic and acetic acid (Bennett et al., 2009; González-Cabaleiro et al., 2013)) and H_2 partial pressures of 120 kPa absolute using equation 7. Calculations were done assuming a reduced:oxidized ferredoxin ratio of 9 and NADH:NAD^+ ratio of 0.1 (Buckel & Thauer, 2013).

$$\Delta G' = \Delta G^{0'} + RTln(Q) \quad (7)$$

where $\Delta G'$ and $\Delta G^{\circ\prime}$ are the Gibbs free energy change of reaction ($J\,mol^{-1}$) at intracellular metabolite concentrations and at standard concentrations, respectively, R is the molar gas constant ($8.31\,J\,mol^{-1}\,K^{-1}$), T is the temperature of reaction (310.15 K) and Q is the reaction quotient.

RESULTS

Clostridium luticellarii requires strict conditions for autotrophic growth

Initially, several attempts were made to transfer *C. luticellarii* from a methylotrophic growth medium as in Petrognani et al. (2020) to the same growth medium without methanol but with H_2 and CO_2 as electron and carbon source. However, the strain repeatedly lost its capacity to grow after approx. three subcultures.

Hence, a systematic experiment was set up to determine the conditions enabling autotrophic growth of *C. luticellarii*. *C. luticellarii* was transferred into pressurized bottles (150 kPa of an 80:20 H_2:CO_2 atmosphere) containing four basal media compositions, all in triplicate. Results showed that autotrophic growth of *C. luticellarii* without a complex nitrogen source (as in media composition (i) and (ii)) was possible to some extent with observable gas consumption, but the culture grew slowly to a low final OD (0.14 ± 0.02 for case (i) and 0.07 ± 0.00 for case (ii)) and lost its ability to grow after approx. 3 subcultures regardless of the concentration of vitamins and trace elements, indicating that the culture was lacking growth factors (Figure 1A). *C. luticellarii* showed faster and more stable growth (across sub cultures) with either 1 g L^{-1} yeast extract or 0.5 g L^{-1} tryptone to a max OD of 0.21 ± 0.00 and 0.18 ± 0.02, respectively (Figure 1A). However, since yeast extract also contains carbohydrates (Tomé, 2021), which makes it unclear whether observed growth was actually autotrophic and might distort the product spectrum towards more reduced products, we decided to use tryptone as complex nutrient source in subsequent experiments. To verify that tryptone did not interfere with the desired autotrophic growth of *C. luticellarii*, we also investigated whether it could support growth without addition of H_2 and CO_2 or other carbon sources and observed no growth (Figure S1). Next, the impact of shaking conditions (to maximize mass transfer from the gas to liquid phase) was assessed by comparing the static incubation of *C. luticellarii* to its incubation on a shaking incubator at 150 rpm. The results of these experiments showed a decreased rate of gas consumption and decreased amount of total gas consumed under shaking conditions compared to static incubations (Figure 1B). Hence, static incubations were used for all subsequent experiments.

Once the growth conditions were established, *C. luticellarii* was first grown under 150 kPa of an 80:20 H_2:CO_2 atmosphere and at initial pH 6.5 to obtain a reference dataset for comparison with other growth conditions. Under these conditions, *C. luticellarii* grew to a maximum OD_{620} of 0.18 ± 0.01 and produced almost exclusively acetic acid to a concentration of 60.46 ± 1.41 mM within 35 days. Beyond acetic acid, only traces of butyric (0.77 ± 0.05 mM) and isobutyric (0.57 ± 0.01 mM) acids were detected (Figure 1C).

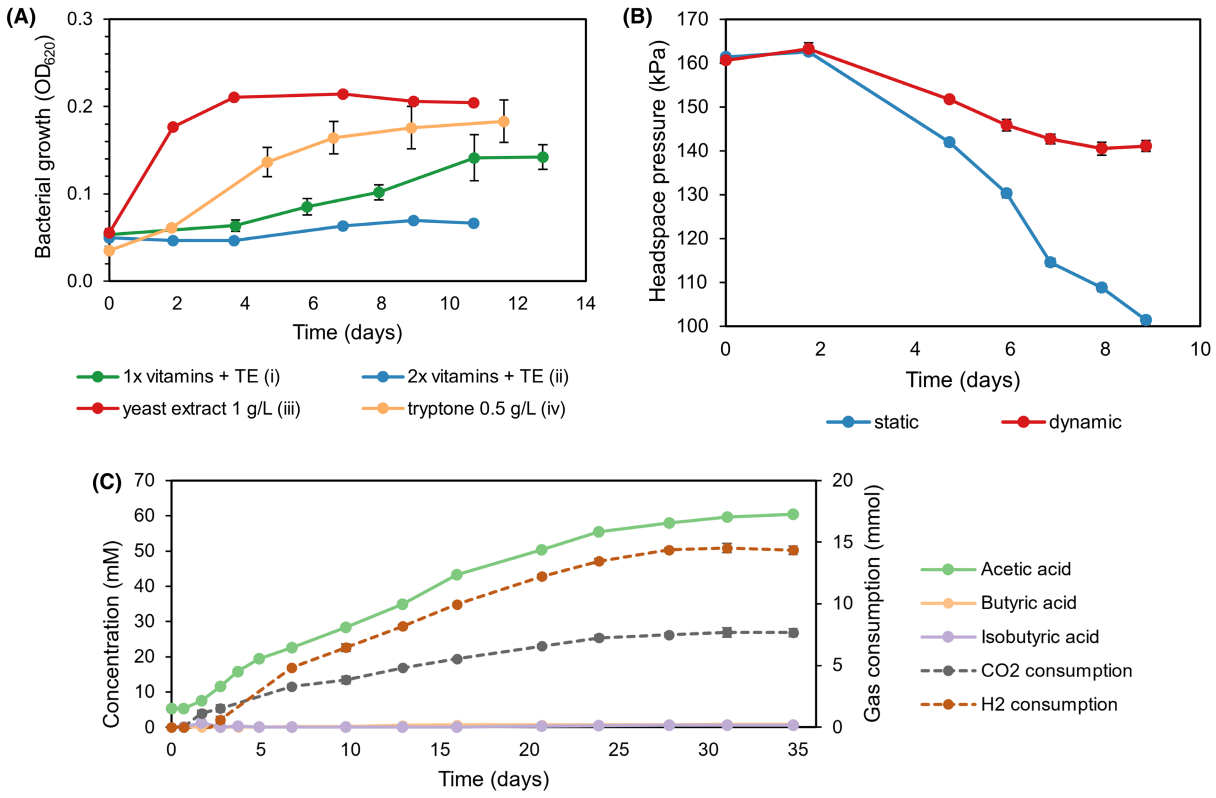

FIGURE 1 (A) Growth curves of the four different conditions tested to determine optimal growth conditions. TE, trace elements. (B) Headspace pressures used as proxy for gas consumption and growth during static incubations and dynamic incubations on a shaker at 150 rpm. (C) Timeseries of product concentrations during autotrophic growth at initial pH 6.5, with 0.5 g L^{-1} tryptone and statically incubated. Error bars represent standard error of three biological replicates.

The effect of acetic and butyric acid on autotrophic isobutyric acid production

In many methylotrophic acetogens capable of producing butyric acid, the concentrations of butyric acid produced from methanol and CO_2 are heavily influenced by the concentrations of metabolic products such as acetic acid (Kremp & Müller, 2020; Pacaud et al., 1986; Petrognani et al., 2020), but their effect on autotrophic growth remains unclear. *C. luticellarii* was grown autotrophically in the presence of 50 mM acetic acid, 50 mM butyric acid or 50 mM isobutyric acid, to assess their individual impact (Figure 2). Supplementation of acetic acid enabled the production of butyric acid and isobutyric acid to near-equimolar concentrations of respectively 8.98 ± 0.91 mM and 9.27 ± 1.32 mM. In terms of selectivity, butyric and isobutyric acid accounted for, respectively, 26 ± 1% and 27 ± 2% of the product spectrum based on electron equivalents contained in the products, with the remaining fraction being acetic acid at a final concentration of 100.61 ± 2.35 mM. When 50 mM of butyric acid was added to the medium, a net decrease in the butyric acid concentration by 16.40 ± 1.80 mM was observed with the concurrent production of 18.06 ± 2.41 mM isobutyric acid, which accounted for 59 ± 6% of the electrons in the product spectrum, alongside acetic acid production to a final concentration of 78.75 ± 4.68 mM. The reversed reaction was also investigated by adding 50 mM isobutyric acid, which resulted in isobutyric acid consumption of 15.84 ± 1.43 mM with a concomitant production of butyric acid up to 13.33 ± 0.82 mM at a selectivity of 57 ± 5% based on electrons in the products. The remaining product spectrum consisted of acetic acid at a final concentration of 70.93 ± 3.32 mM. Interestingly, the lag phase when isobutyric acid was added was much longer than with any of the other organic acids (6 days compared with 1–2 days for other organic acids, Figures S2 and S3). In an attempt to further increase isobutyric acid concentrations, both acetic and butyric acid were added at 50 mM each. This resulted again in butyric acid consumption, albeit lower than previously observed at a net consumption of 9.62 ± 0.98 mM, with isobutyric acid production up to similar concentrations as the condition with only butyric acid (net production of 18.71 ± 3.15 mM). The discrepancy between the butyric acid consumed and isobutyric acid produced shows that isobutyric acid might not only be produced from the added exogeneous butyric acid, but part of its production must also come from consumed H_2 and CO_2 and/or the initially supplied acetic acid. Nonetheless, the main product was still acetic acid, with a net production of 59.16 ± 1.46 mM. Alcohols were not detected in any of the tested conditions.

The effect of pH on autotrophic growth of *C. luticellarii*

In some acetogens, mildly acidic pH stimulates the production of alcohols and longer chain carboxylic acids (Vees et al., 2020; Worden et al., 1991). Therefore, the effect of pH on the growth of *C. luticellarii* was assessed first without any carboxylic acid additions and with the addition of 50 mM acetic acid The pH values tested were 5.5 and 6.5 and were controlled throughout the experiments between 5.0–5.5 and 6.0–6.5, respectively. These experiments were conducted using a higher inoculum ratio (25% instead of 10%) to minimize the duration of the lag phase due to a potentially suboptimal pH for growth (Petrognani et al., 2020). However, this affected the initial OD and concentrations of products so caution is advised in comparing this data to those of the other experiments.

The autotrophic growth of *C. luticellarii* at pH 5.5 without any additions showed a similar maximum achieved OD (0.24 ± 0.02) compared to pH 6.5 (0.24 ± 0.03), but a lower total H_2 and CO_2 consumption (8.74 ± 0.69 mmol H_2 and 3.10 ± 0.29 mmol CO_2 at pH 5.5 compared with 15.03 ± 1.47 mmol H_2 and 5.95 ± 0.37 mmol CO_2 at pH 6.5) (Figure 3). Additionally, butyric and isobutyric acid production started earlier at pH 5.5 and reached

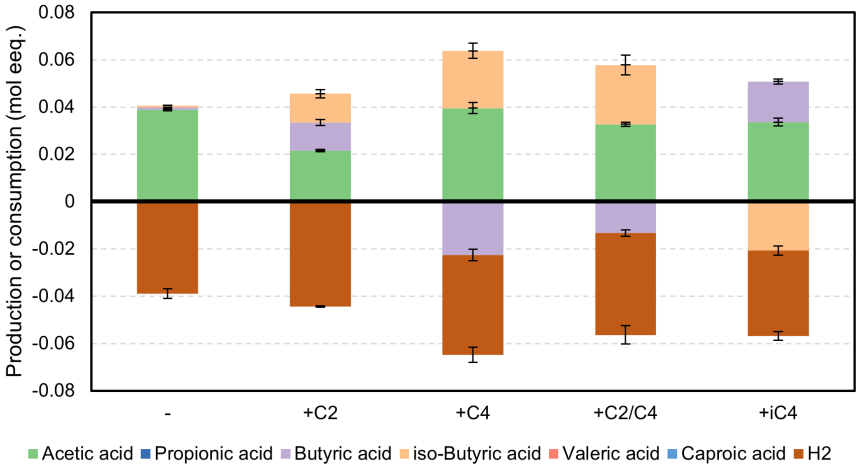

FIGURE 2 Electron balance of growth of *C. luticellarii* at initial pH 6.5 with different organic acids (all supplied at 50 mM) in presence of H_2 and CO_2. Net production is shown on the positive *y* axis and net consumption is on the negative *y* axis. Values are calculated as absolute amounts of net consumed/produced electron equivalents (eeq.) in mol eeq. C2 = acetic acid, C4 = butyric acid, iC4 = isobutyric acid.

a higher concentration of, respectively, 2.36 ± 0.51 mM and 2.79 ± 0.70 mM (compared to 2.22 ± 0.55 mM butyric acid and 1.98 ± 0.40 mM isobutyric acid at pH 6.5) (Figure S5). The final global C4 (C4 + iC4) selectivity was 27 ± 9% at pH 5.5 compared to 13 ± 2% at pH 6.5, indicating low pH favoured chain elongation. Growth at pH 5.5 with 50 mM initial acetic acid concentrations resulted in a final OD of 0.22 ± 0.02. The total amount of gas consumed (10.21 ± 0.86 mmol H_2 and 3.74 ± 0.34 mmol CO_2) was similar to growth at pH 5.5 without initial acetic acid, but the selectivity of C4 products (butyric and isobutyric acid combined) was higher at 42 ± 4% indicating the effect of pH and elevated acetic acid concentrations is cumulative (Figure 3). The selectivity for C4 compounds at pH 5.5 with 50 mM acetic acid was, however, slightly lower than at pH 6.5 with 50 mM acetic acid (53 ± 3%) as described in The effect of acetic and butyric acid on autotrophic isobutyric acid production although those experiments were done at a lower inoculum ratio and uncontrolled pH which may have affected the outcome.

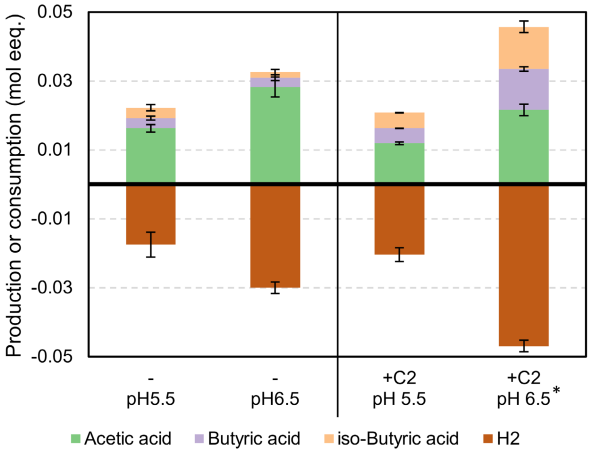

FIGURE 3 Electron balance of growth of *C. luticellarii* on H_2 and CO_2 at pH 6.5 and pH 5.5 with and without acetic acid (C2, 50 mM). Net production is shown on the positive *y* axis and net consumption is on the negative *y* axis. Values are calculated as absolute amounts of net consumed/produced electron equivalents (eeq.) in mol eeq. *This condition was run without pH control and at inoculum ratio 10% as depicted in Figure 2. The other conditions presented were done at controlled pH and inoculum ratio 25%. C_2 = acetic acid.

Impact of the additions of valeric and caproic acid on the metabolism of *C. luticellarii*

The production of isobutyric acid observed during growth at elevated butyric acid concentrations strongly suggests the occurrence of bio-isomerisation. To assess whether *C. luticellarii* is also capable of forming isomers of other linear carboxylic acids such as valeric and caproic acid, *C. luticellarii* was grown in presence of either 25 mM of valeric acid or 25 mM of caproic acid (Figure S4). Neither additions resulted in production of their respective isomers. However, *C. luticellarii* did consume 6.85 ± 1.31 mM of valeric acid with concurrent production of 5.83 ± 0.51 mM of propionic acid. In the valeric acid experiment, its consumption accounted for 25 ± 3% of the total electrons consumed (H_2 and valeric acid combined) and H_2 and valeric acid were consumed simultaneously, showing that *C. luticellarii* grew mixotrophically. The main product was acetic acid at a final concentration of 66.91 ± 7.44 mM (Figure 4, 25 mM). Caproic acid addition at 25 mM led to a significantly lower consumption of H_2 and CO_2 which was only used for the production of 50.16 ± 1.31 mM acetic acid (Figure S4).

The near-equimolar nature of the conversion of valeric acid to propionic acid points at valeric acid being

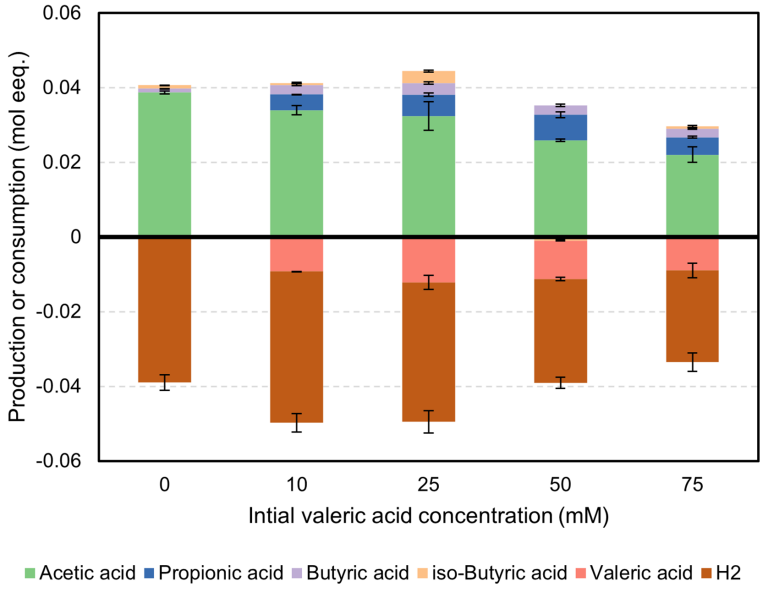

FIGURE 4 Electron balance of growth of *C. luticellarii* at different initial valeric acid concentrations in presence of H_2 and CO_2. Net production is shown on the positive *y* axis and net consumption is on the negative *y* axis. Values are calculated as absolute amounts of net consumed/produced electron equivalents (eeq.) in mol eeq.

oxidized via the β-oxidation pathway even though hydrogen partial pressures here (>100 kPa) exceed the limits for organic acid oxidation commonly reported in literature related to chain elongation and/or anaerobic digestion by several orders of magnitude (approx. 1–300 Pa (Ge et al., 2015; Stams, 1994)). To gain further insight into the oxidation of valeric acid under high H_2 partial pressures, *C. luticellarii* was grown under increasing concentrations of valeric acid (Figure 4, Figure S6). At initial concentrations of 10, 50 and 75 mM valeric acid, respectively, 4.95 ± 0.02 mM, 5.52 ± 0.28 mM and 4.84 ± 1.22 mM of valeric acid was consumed and 4.28 ± 0.08 mM, 5.82 ± 0.12 mM and 4.68 ± 0.34 of propionic acid was produced (Figure 4). The initial concentration of valeric acid thus did not have a large effect on the amount of valeric acid consumed, but consumption of valeric acid and production of propionic acid again occurred in nearly equimolar amounts in all cases. Additionally, valeric acid exerted a toxic effect on *C. luticellarii* from 50 mM onwards since the gas uptake decreased from 20.25 ± 1.28 mmol H_2 and 8.28 ± 0.69 mmol CO_2 at 10 mM valeric acid to 12.62 ± 1.23 mmol H_2 and 5.28 ± 0.56 mmol at 75 mM valeric acid, and the maximum OD decreased from 0.17 ± 0.01 at 10 mM valeric acid to 0.08 ± 0.00 at 75 mM valeric acid.

A thermodynamic analysis of organic acid oxidation was performed to assess why and how *C. luticellarii* is able to oxidize valeric acid to propionic acid and acetic acid under an atmosphere with elevated H_2 partial pressure. Two cases were calculated: (1) Oxidation of valeric acid assuming that protons are used as final electron sink to produce H_2 and (2) Oxidation of valeric acid with using intracellular electron carriers as electron acceptors, whose electrons are internally reused to, for example, fuel the WLP. For both cases, the energy conservation mechanism considered is the production of one ATP through substrate-level phosphorylation per molecule of valeric acid oxidized, thus a global Gibbs free energy (ΔG′) of the process of −50 kJ/mol valeric acid was used as threshold for process thermodynamic feasibility (Buckel & Thauer, 2013; González-Cabaleiro et al., 2015). In Case 1, the oxidation with co-production of H_2 at pH 6.5 and 120 kPa of H_2 has a ΔG′ of +25 kJ/mol valeric acid deeming it thermodynamically unfeasible. The reaction only becomes feasible at pH 6.5 at extremely low H_2 partial pressures ($<6 \times 10^{-2}$ Pa). The pathway does become more favourable with increasing pH, but never surpasses the threshold of thermodynamic feasibility within the range of pH 5–7 (Figure 5A). However, assuming case 2, the reaction is feasible at pH 6.5 and under 120 kPa of H_2 with a ΔG′ of −59.5 kJ/mol valeric acid and is thus also exergonic enough to allow for ATP production. The thermodynamic feasibility of Case 2 is also affected by pH, decreasing its feasibility with decreasing pH, and becomes unfavourable at pH values below approximately 5.7 (Figure 5A). Since the calculations that led to this value hinge on several assumptions (e.g. intracellular metabolite concentrations, reduced:oxidized electron carrier ratios, etc.), the value should be taken as an indication and not an absolute cut-off.

To validate the conclusions of the thermodynamic calculations on the effect of pH on valeric acid oxidation, *C. luticellarii* was grown with 25 mM valeric acid at controlled pH 6.5 and 5.5 (Figure 5B and Figure S7). The pH had a substantial effect on the fraction of valeric acid oxidized. At pH 5.5, 9 ± 3% of the initially supplied valeric acid was consumed, while at pH 6.5 this fraction was 3 times higher at 31 ± 3%. Taking into account the total substrate consumption, valeric acid consumption represented 25 ± 4% of the electrons consumed (H_2 and valeric acid combined) at pH 6.5, whereas this

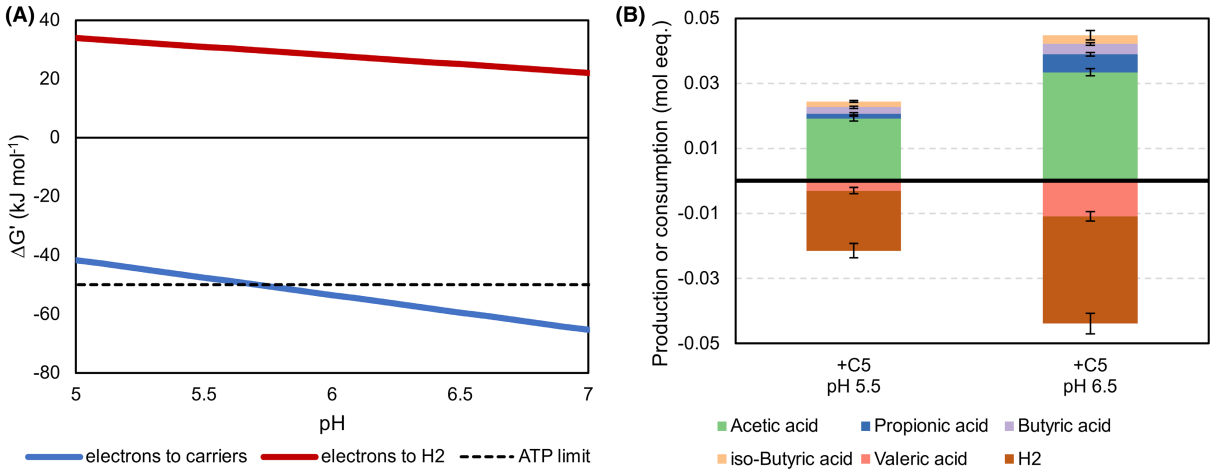

FIGURE 5 (A) Thermodynamic calculations of valeric acid oxidation comparing the transfer of electrons to carriers that can be regenerated in the WLP, with the regeneration of electron carriers via H_2 production. (B) The effect of pH on valeric acid oxidation. Net production is shown on the positive *y* axis and net consumption on the negative *y* axis. Values are calculated as absolute amounts of net consumed/produced electron equivalents (eeq.) in mol eeq.

was 14 ± 4% at pH 5.5. Similar trends were observed for propionic acid production, which was higher at pH 6.5. This suggests oxidation still occurred to some extent, but was less favourable at low pH as predicted by the thermodynamic analysis. To gain further insight into the oxidation, *C. luticellarii* was incubated in presence of 25 mM valeric, but absence of H_2 by flushing with a 90:10 N_2:CO_2 gas mixture. No growth was observed under these conditions and valeric acid was not consumed (Figure S8).

DISCUSSION

Clostridium luticellarii requires complex nutrients and a low-shear environment to grow on H_2 and CO_2

While *C. luticellarii* was capable of growing autotrophically, it required tryptone or yeast extract and static conditions to grow reproducibly across sub cultures. The necessity of complex nutrients (e.g. yeast extract and/or tryptone) to enable autotrophic growth of acetogens has been reported earlier. For example, Martin et al. (2016) tested the dependence of six different autotrophic strains of acetogens on yeast extract and only managed to grow three of them without a complex nutrient source. This can be connected to the fact that the metabolism of acetogens often runs close to the thermodynamic limit of life due to the low availability of energy under autotrophic conditions, potentially also impacting their capacity to synthesize all cell constituents de novo (Schuchmann & Müller, 2014). Therefore, many studies focusing on medium development for acetogens and studies characterizing the autotrophic growth of acetogens have used yeast extract as a complex nutrient source providing vitamins, trace elements and amino acids (Arslan et al., 2019; Chang et al., 2007; Groher & Weuster-Botz, 2016a, 2016b; Litty & Müller, 2021). However, regardless of the source of yeast extract, at least 7%–13% of it is composed of readily degradable carbon sources such as carbohydrates (Tomé, 2021), which can be converted to organic acids. This may distort the results of some studies where, comparatively, the electron equivalents potentially stemming from the carbohydrates in yeast extract are higher than the electron equivalents coming from the actual substrates under study. We advocate the use of moderate concentrations of tryptone over yeast extract whenever possible in studies characterizing production capacities of microorganisms since tryptone is a lean source of amino acids that does not usually support growth in absence of other substrates as shown in *Clostridium luticellarii* requires strict conditions for autotrophic growth. Additionally, where the use of yeast extract is inevitable, a close eye should be kept on whether electron and carbon balances close (i.e. equal amounts of carbon and electrons consumed as produced) to minimize the interference of yeast extract on the studied metabolism. Here, we chose to supplement growth media with 0.5 g L^{-1} tryptone instead of 1 g L^{-1} yeast extract, and managed to reproducibly grow *C. luticellarii* without any addition of carbohydrates (Figure 1).

Results also indicated that *C. luticellarii* consumes gas much slower and to a lesser extent under shaking conditions than when statically incubated. This result is counterintuitive, since shaking increases the gas–liquid mass transfer rate and thus the substrate availability for the bacteria but it grows better under passive diffusion. One potential hypothesis may be that *C. luticellarii* is sensitive to the shear stress induced by shaking conditions. Although this is not uncommon in anaerobic bacteria, the underlying mechanism remains unclear (Jonczyk et al., 2013). Scaling up gas fermentation with shear sensitive *C. luticellarii* may prove a challenge since classic approaches such as CSTRs may introduce too much shear due to mixing, and bubble column or gas lift reactors may induce too much shear due to bubble flow. Attractive alternatives are low-shear reactor designs such as the bubble-less hollow fibre membrane biofilm reactors or the exclusive use of CO_2-derived liquid molecules (e.g. methanol) (Elisiário et al., 2021; Petrognani et al., 2020).

Autotrophic isobutyric and butyric acid production is stimulated by elevated acetic acid concentrations

Autotrophic growth of *C. luticellarii* at pH 6.5 was mainly characterized by acetic acid production, which is the dominant product in the majority of acetogens (Bengelsdorf et al., 2018), accompanied by traces of butyric and isobutyric acid. These results are similar to those reported for other acetogens capable of producing traces of butyric acid when grown on H_2 and CO_2, such as *B. methylotrophicum* (Lynd & Zeikus, 1983), *E. limosum* KIST612 (Litty & Müller, 2021), *B. hydrogenotrophica* DSM 10507, *C. magnum* DSM 2767 and *E. aggregans* DSM 12183 (Groher & Weuster-Botz, 2016a). It also aligns well with the findings of González-Cabaleiro et al. (2013), where chain elongation to butyric acid with H_2 as electron donor was found to be kinetically bottlenecked in the first step of the reverse β-oxidation pathway due to the unfeasibly low internal acetoacetyl-CoA levels required to drive the condensation reaction of two acetyl-CoA molecules.

Increasing the initial acetic acid levels from 0 to 50 mM increased the selectivity of C4 compounds (sum of butyric and isobutyric acid) from 5 ± 1% to 53 ± 3%. Similar selectivity shifts towards butyric

acid at elevated levels of acetic acid have been reported for methanol-based studies with *C. luticellarii*, but also with *E. limosum* and *B. methylotrophicum* (Lynd & Zeikus, 1983; Pacaud et al., 1986; Petrognani et al., 2020). It has been hypothesized that high acetic acid concentrations exert a feedback inhibition on its production, thereby redirecting carbon flux from acetyl-CoA to reverse β-oxidation instead of acetic acid (Kremp & Müller, 2020), but it remains unclear how this alleviates the kinetic bottleneck proposed by González-Cabaleiro et al. (2013).

Isobutyric acid is likely formed by a selective isomerization of butyric acid

In our experiments, isobutyric and butyric acids were co-produced during the autotrophic growth of *C. luticellarii* at pH 5.5 and at elevated concentrations of acetic acid (Figure 2). Additionally, autotrophic growth at elevated butyric acid concentrations resulted in its consumption and the concomitant production of isobutyric acid at nearly equimolar amounts. This aligns with earlier work by Petrognani and co-workers, who showed that isobutyric acid production from methanol and CO_2 is stimulated by elevated butyric acid concentrations, suggesting an interconversion of both compounds (Petrognani et al., 2020). The most plausible hypothesis is that *C. luticellarii* isomerizes butyric acid to isobutyric acid. This mechanism has been suggested before for *C. luticellarii* growing on methanol and CO_2 by Petrognani et al. (2020) and by Liu et al. (2020), who isolated a closely related *Clostridium* sp. BL3 producing butyric and isobutyric acid from lactic acid. However, neither study reported net butyric acid consumption alongside isobutyric acid production to fully support this hypothesis. The suggested pathway in these studies consists of isomerization of n-butyryl-CoA (coming from n-butyric acid activation or from in situ production through reverse β-oxidation) to isobutyryl-CoA by a butyryl-CoA:isobutyryl-CoA mutase (BM) and final conversion of isobutyryl-CoA to isobutyric acid by an isobutyryl-CoA:acetate CoA transferase (Liu et al., 2020; Petrognani et al., 2020). Homologues for all enzymes involved are present in the *C. luticellarii* genome (Liu et al., 2020). All steps of the isomerisation pathway seem to be reversible, as supported by the observed consumption of isobutyric acid alongside production of butyric acid at nearly equimolar amounts (Figure 2 and Figure S3). However, *C. luticellarii* showed a much longer lag phase when grown on isobutyric acid compared to butyric acid, which is counterintuitive assuming the same enzymes are used in both directions. The mechanism behind the long lag phase thus remains unclear.

To check whether *C. luticellarii* could also convert valeric acid or caproic acid to their respective isomers, autotrophic growth at elevated concentrations of valeric acid and caproic acid was tested. Neither of the added organic acids resulted in occurrence of their respective isomers. This aligns with the myriad of chain elongation studies that reported significant iso-butyric acid production (but not iso-caproic acid production) in mixed and pure culture systems engineered for butyric and caproic acid production (Huang et al., 2020; Liu et al., 2020; Mariën et al., 2022), and the lack of studies reporting significant iso-valeric acid production in similar studies aiming for valeric acid production (Allegue et al., 2022; de Smit et al., 2019; Ganigué et al., 2019). This could be either due to the (iso-)acids not being transported through the cell membrane, the acids not being activated to their respective CoA form, and/or the BM of *C. luticellarii* being specific for (iso)butyric acid. The transport into the cell and activation of the acid is likely not preventing production of isovaleric acid (or isomers of other carboxylic acids), since oxidation of valeric acid to propionic and acetic acid was observed, for which valeric acid needs to enter the cell and requires activation to valeryl-CoA. The likely bottleneck is the specificity of the BM enzyme since several studies report acyl-CoA mutases to have a strict substrate specificity (Cracan & Banerjee, 2012). Purification and characterization of the *C. luticellarii* BM could further prove this hypothesis.

The ecological reason behind the interconversion of butyric acid to isobutyric acid (and vice versa) remains obscure since no free energy is released during the isomerization. Liu et al. (2020) and Allison (1978) argued that bacteria may convert n-butyric acid to isobutyric acid to maintain a high isobutyric acid pool for the synthesis of valine in media poor in amino acids. Here, the medium *C. luticellarii* was grown on contains 0.5 g L^{-1} tryptone, providing a readily accessible source of amino acids (albeit at a low concentration). This suggests that either the mechanism may not be directly regulated by amino acid availability or another ecological reason is behind the mechanism. Others have suggested that isomerization is a way to deal with high concentrations of toxic n-butyric acid by converting it to less toxic isobutyric acid, and thus allowing microorganisms to continue generating energy through butyric acid production (Chen et al., 2017). The production of isobutyric acid was not only observed here at high butyric acid concentrations but was also observed at low butyric acid concentrations (<10 mM) concomitantly with butyric acid production, casting doubt on the toxicity hypothesis. Additionally, neither of the proposed hypotheses explains the benefit of reverse isomerisation (i.e. isobutyric acid to butyric acid). Exploration of the proteome and metabolome of *C. luticellarii* under different environmental conditions may provide further answers as to why this isomerisation occurs.

pH drives metabolic flexibility between the reductive and oxidative direction of the autotrophic reverse β-oxidation pathway

In our work, pH was identified to be a controlling parameter between reductive and oxidative processes in *C. luticellarii*: (1) circumneutral pH (~6.5) increased the fraction of valeric acid oxidized, and (2) mildly acidic pH (≤5.5) increased the selectivity for butyric and isobutyric acid production by stimulating reverse β-oxidation. While both processes are seemingly different, they are in fact the same pathway running in opposite directions.

Thermodynamic calculations and the results presented in this article show that *C. luticellarii* is unequivocally able to oxidize valeric acid to acetic and propionic acid at circumneutral pH under a hydrogen partial pressure of 120 kPa, contradicting at first glance established literature reporting the blockage of organic acid oxidation at H_2 partial pressures as low as 1 Pa (Ge et al., 2015; Stams, 1994). Organic acid oxidation is usually considered to be coupled with H_2 formation. This implies that the NAD^+ reduced to NADH (NAD^+/NADH $E' = -280$ mV (Buckel & Thauer, 2013)) during oxidation must be reoxidised with protons as electron sink and hence the production of H_2, which is thermodynamically unfeasible at high H_2 partial pressures (H^+/H_2 $E' = -340$ mV at 250 Pa H_2 which is even considerably lower than H_2 pressures used in this study (Schuchmann & Müller, 2014; Stams, 1994)). A similar case of oxidation in seemingly unfavourable conditions has been reported in the model chain elongator *C. kluyveri*. For years, scientists had hypothesized on how *C. kluyverii* is able to oxidize ethanol (which yields NADH) during reverse β-oxidation given that the strain internally accumulates H_2 up to a partial pressure of 1 bar (Li et al., 2008; Seedorf et al., 2008). The answer to this question was that NADH can be reoxidised in the reverse β-oxidation pathway without generation of H_2 (Li et al., 2008; Seedorf et al., 2008). We argue that *C. luticellarii* may be able to carry out organic acid oxidations in a similar way where NAD^+ is likely regenerated by NADH oxidation in one of the reducing steps of the methyl branch in the WLP (i.e. reduction of CO_2 to formate, or the sequential reductions of methenyl-THF to methylene-THF and methyl-THF) and not by H_2 production. However, currently very little is known about the electron carriers used in the Wood–Ljungdahl Pathway of *C. luticellarii*, making it difficult to prove this hypothesis at this point. Further characterization of the cofactors used in the individual reduction steps would allow performing a thermodynamic analysis over the entire metabolism (i.e. combination of the Wood–Ljungdahl pathway and organic acid oxidation) and elucidating the mechanism. Oxidation of organic acids simultaneously with autotrophic metabolism may also offer another advantage to *C. luticellarii* by providing an efficient alternative for ATP generation from reduced ferredoxin, which is produced during H_2 oxidation. During autotrophic metabolism, acetogens usually generate ATP from the excess reduced ferredoxin produced during H_2 oxidation by oxidizing it in the Ferredoxin:NAD^+ oxidoreductase complex (RnF), which uses the released energy to generate an ion motive force that drives ATP synthesis via an ATPase (Schuchmann & Müller, 2014). The oxidation of valeric acid offers an alternative to this because the enzyme complex catalysing the oxidation of valeryl-CoA needs reduced ferredoxin in an electron confurcation process, where electrons from reduced ferredoxin and valeryl-CoA reduce NAD^+ to NADH. Hence, the investment of two reduced ferredoxin (assumed monovalent here) in this case yields 3 NADH and one full ATP (Equation 5), while the classic RnF–ATPase route only produces one NADH and ~0.50–0.67 ATP from the same ferredoxin investment (Schuchmann & Müller, 2014). In this sense, we argue that those acetogens with substrate flexibility (i.e. the ability to (co-)oxidize organic acids even at high H_2 partial pressures) may have a competitive advantage against those who cannot, since they may use more efficiently the available reduced ferredoxin and conserve more energy in the form of ATP. The use of valeric acid oxidation as an alternative way to regenerate ferredoxin is also supported by the fact that valeric acid is not oxidized in absence of H_2, since in that case there is no direct source of reduced ferredoxin. This suggests that valeric acid oxidation is a secondary metabolism, depending on other substrates (here H_2 that drives the WLP) to support it. However, reduced ferredoxin could theoretically be indirectly generated through investing ~0.5–0.67 of the ATP formed in valeric acid oxidation via the reversal of the RnF–ATPase route, thereby consuming one NADH for the production of two reduced ferredoxin. In this way, valeric acid could be oxidized with the remaining two NADH being reoxidized to NAD^+ through H_2 production, maintaining a final ATP yield of 0.33–0.5 ATP per valeric acid oxidized. It is unclear why *C. luticellarii* is unable to do so to sustain growth in absence of H_2.

While the experiments presented here focused on valeric acid oxidation for which the degradation product propionic acid is easily detectable, a similar case can be made for the oxidation of other organic acids such as butyric acid. However, we were unable to prove butyric acid oxidation here due to (i) its degradation product being acetic acid which is also the main metabolic end product from the WLP, and (ii) butyric acid is also consumed for the production of isobutyric acid. Both processes occurring simultaneously with butyric acid oxidation make it difficult to accurately follow the carbon flux, hence, follow-up

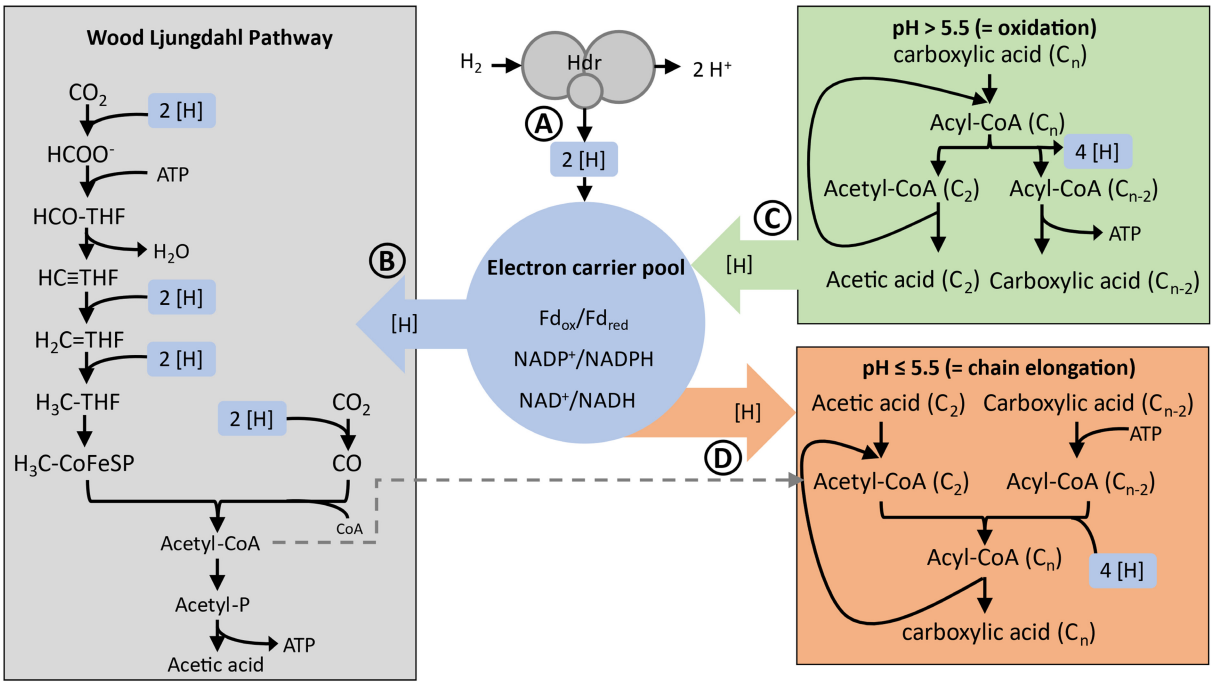

FIGURE 6 The hypothetical direction of electron flow in the metabolism of *C. luticellarii* driven by changes in pH. (A) *C. luticellarii* oxidizes hydrogen to generate reducing equivalents that contribute to the reduction of the electron carrier pool. (B) Reduced electron carriers are used in the WLP and for energy generation. The WLP serves as the central carbon fixation pathway regardless of pH. (C) Whenever pH is high enough (>~5.5) and butyric acid ($n=4$) or valeric acid ($n=5$) is present, they may be oxidized in parallel with the WLP to generate additional electron equivalents that contribute to the reduction of the electron carrier pool, as well as 1 ATP per organic acid oxidized. (D) When pH is low (≤~5.5) oxidation of organic acids is thermodynamically unfavourable and the pathway reverses to the direction of reverse β-oxidation, now becoming an electron-consuming pathway instead of an electron-generating pathway. Fd, ferredoxin; Hdr, hydrogenase.

studies using isotope-labelled butyric acid may shed further light on this.

The thermodynamic analysis identified pH as key parameter in Impact of the additions of valeric and caproic acid on the metabolism of *C. luticellarii*: at mildly acidic pH (<~5.5), *C. luticellarii* shifts its metabolism towards producing more of the chain elongation products butyric and isobutyric acid. Similar shifts towards chain elongation products have been reported by Worden et al. (1991) who observed a four-fold increase in butyric acid production from CO by *Butyribacterium methylotrophicum* when shifting pH from 6.8 to 6.0. To explain the effect of pH on chain elongation and oxidation, we suggest the following hypothesis (Figure 6): at circumneutral pH (~6.5), *C. luticellarii* can leverage its substrate flexibility to oxidize H_2 and organic acids (e.g. butyric or valeric acid) simultaneously, thereby generating reduced electron carriers and allowing a higher ATP yield than when oxidizing H_2 alone due to the mechanism explained above. As long as pH remains high enough (>~5.5), *C. luticellarii* can run the Wood–Ljungdahl Pathway and organic acid oxidation simultaneously. At mildly acidic pH (≤~5.5), the oxidation of organic acids becomes less favourable and upon surpassing a thermodynamic threshold, the oxidation reverses and operates in the reductive direction (i.e. chain elongation) via reverse β-oxidation (i.e. condensing and reducing two acetyl-CoA molecules to produce butyric and isobutyric acid). This process represents a net consumption of electron equivalents coming from the oxidation of H_2 and is driven by the production of reduced ferredoxin (via electron bifurcation in the crotonyl-CoA reduction) which can be used for additional ATP generation through its oxidation in the RnF complex. This remarkable metabolic flexibility shows how adapted *C. luticellarii* is to operate at the limit of thermodynamic viability since it is able to reverse the direction of carbon flux in its metabolism to generate additional ATP from the products of its autotrophic metabolism depending on the prevailing environmental conditions. Additionally, to the best of our knowledge this represents the first report of an acetogen with the capacity to use the (reverse) β-oxidation in opposite directions according to a change of pH while conserving energy regardless of the direction.

CONCLUSIONS

This study investigated the autotrophic growth of *C. luticellarii* by identifying the necessary growth conditions and examining the effects of metabolite levels and pH on butyric and isobutyric acid titers and

selectivity. Our experiments concluded that *C. luticellarii* requires the addition of complex nutrient sources and the absence of shaking conditions for autotrophic growth. To steer product selectivity, pH was identified as a key parameter governing the direction of metabolic fluxes. At circumneutral pH (>5.5), acetic acid is the sole metabolic end product and, additionally, *C. luticellarii* shows the particular ability to co-oxidize organic acids such as valeric acid under high H_2 partial pressures (>1 bar). Conversely, mildly acidic pH (<5.5) stimulates the production of butyric and isobutyric acid. Additionally, elevated acetic acid concentrations stimulated butyric and isobutyric acid production up to a maximum combined selectivity of 53 ± 3%. Finally, our results suggest that isobutyric acid is produced by a reversible isomerization of butyric acid, but valeric and caproic acid are not isomerized by *C. luticellarii*. While this study positions *C. luticellarii* and its uniquely flexible metabolism producing butyric and isobutyric acid from H_2 and CO_2 as a promising candidate for industrial biotechnological applications, further research should focus on improving yields and production rates on reactor-scale. Overall, the combined insights reported here can inform the future efforts to optimize and scale-up the production of valuable chemicals from CO_2 using *C. luticellarii*.

AUTHOR CONTRIBUTIONS

Quinten Mariën: Conceptualization (lead); data curation (lead); formal analysis (lead); funding acquisition (lead); investigation (lead); methodology (lead); validation (lead); visualization (lead); writing – original draft (lead). **Alberte Regueira:** Conceptualization (supporting); investigation (supporting); methodology (supporting); supervision (supporting); writing – review and editing (equal). **Ramon Ganigué:** Conceptualization (supporting); funding acquisition (supporting); methodology (supporting); resources (lead); supervision (lead); writing – review and editing (equal).

ACKNOWLEDGMENTS

QM was supported by the Research Foundation of Flanders (Fonds Wetenschappelijk Onderzoek Vlaanderen, FWO) [grant number 1SC5722N]. A.R. acknowledges the support of the Xunta de Galicia through a postdoctoral fellowship [ED481B-2021-012]. A.R. belongs to a Galician Competitive Research Group [GRC ED431C 2021/37], cofounded by ERDF (UE). RG was supported by the Special Research Fund of Ghent University [BOF19/STA/044].

CONFLICT OF INTEREST STATEMENT

The authors declare to have no conflict of interest.

DATA AVAILABILITY STATEMENT

All data can be made available upon request to the corresponding author.

ORCID

Ramon Ganigué https://orcid.org/0000-0002-9564-0195

REFERENCES

Abubackar, H.N., Veiga, M.C. & Kennes, C. (2012) Biological conversion of carbon monoxide to ethanol: effect of pH, gas pressure, reducing agent and yeast extract. *Bioresource Technology*, 114, 518–522.

Alberty, R.A. (2003) *Thermodynamics of biochemical reactions*. Hoboken, NJ: Wiley-Interscience.

Allegue, T., Rafay, R., Chandran, S., Amin, S.A., Fowler, S.J. & Rodríguez, J. (2022) Lactate addition boosts valerate yields in granular mixed culture carbohydrate fermentation. *Journal of Environmental Chemical Engineering*, 10, 108869.

Allison, M.J. (1978) Production of branched-chain volatile fatty acids by certain anaerobic bacteria. *Applied and Environmental Microbiology*, 35, 872–877.

Arslan, K., Bayar, B., Nalakath Abubackar, H., Veiga, M.C. & Kennes, C. (2019) Solventogenesis in *Clostridium aceticum* producing high concentrations of ethanol from syngas. *Bioresource Technology*, 292, 121941.

Battistuzzi, G., D'Onofrio, M., Borsari, M., Sola, M., Macedo, A.L., Moura, J.J.G. et al. (2000) Redox thermodynamics of low-potential iron-sulfur proteins. *Journal of Biological Inorganic Chemistry*, 5, 748–760.

Bellei, M., Battistuzzi, G., Wu, S., Mansy, S.S., Cowan, J.A. & Sola, M. (2010) Control of reduction thermodynamics in [2Fe–2S] ferredoxins. *Journal of Inorganic Biochemistry*, 104, 691–696.

Bengelsdorf, F.R., Beck, M.H., Erz, C., Hoffmeister, S., Karl, M.M., Riegler, P. et al. (2018) Bacterial anaerobic synthesis gas (syngas) and CO_2+H_2 fermentation. *Advances in Applied Microbiology*, 103, 143–221.

Bennett, B.D., Kimball, E.H., Gao, M., Osterhout, R., Van Dien, S.J. & Rabinowitz, J.D. (2009) Absolute metabolite concentrations and implied enzyme active site occupancy in *Escherichia coli*. *Nature Chemical Biology*, 5, 593–599.

Boot-Handford, M.E., Abanades, J.C., Anthony, E.J., Blunt, M.J., Brandani, S., Mac Dowell, N. et al. (2014) Carbon capture and storage update. *Energy and Environmental Science*, 7, 130–189.

Buckel, W. & Thauer, R.K. (2013) Energy conservation via electron bifurcating ferredoxin reduction and proton/Na+ translocating ferredoxin oxidation. *Biochimica et Biophysica Acta – Bioenergetics*, 1827, 94–113.

Calvo, D.C., Luna, H.J., Arango, J.A., Torres, C.I. & Rittmann, B.E. (2022) Determining global trends in syngas fermentation research through a bibliometric analysis. *Journal of Environmental Management*, 307, 114522.

Chang, I.S., Kim, D., Kim, B.H. & Lovitt, R.W. (2007) Use of an industrial grade medium and medium enhancing effects on high cell density CO fermentation by *Eubacterium limosum* KIST612. *Biotechnology Letters*, 29, 1183–1187.

Chen, W.-S., Huang, S., Strik, D.P. & Buisman, C.J. (2017) Isobutyrate biosynthesis via methanol chain elongation: converting organic wastes to platform chemicals: isobutyrate production from organic waste using a mixed culture fermentation. *Journal of Chemical Technology and Biotechnology*, 92, 1370–1379.

Claassens, N.J., Cotton, C.A.R., Kopljar, D. & Bar-Even, A. (2019) Making quantitative sense of electromicrobial production. *Nature Catalysis*, 2, 437–447.

Cracan, V. & Banerjee, R. (2012) Novel B_{12} -dependent acyl-CoA mutases and their biotechnological potential. *Biochemistry*, 51, 6039–6046.

de Smit, S.M., de Leeuw, K.D., Buisman, C.J.N. & Strik, D.P.B.T.B. (2019) Continuous n-valerate formation from propionate and

methanol in an anaerobic chain elongation open-culture bioreactor. *Biotechnology for Biofuels*, 12, 132.
Drake, H.L. (1995) *Acetogenesis*. New York, NY: Chapman & Hall.
European Commission, Joint Research Centre, Olivier, J., Guizzardi, D., Schaaf, E. et al. 2021 *GHG emissions of all world : 2021 report*, Publications Office of the European Union. https://data.europa.eu/doi/10.2760/173513
Elisiário, M.P., De Wever, H., Van Hecke, W., Noorman, H. & Straathof, A.J.J. (2021) Membrane bioreactors for syngas permeation and fermentation. *Critical Reviews in Biotechnology*, 42, 1–17.
Fernández-Naveira, Á., Abubackar, H.N., Veiga, M.C. & Kennes, C. (2016) Efficient butanol-ethanol (B-E) production from carbon monoxide fermentation by *Clostridium carboxidivorans*. *Applied Microbiology and Biotechnology*, 100, 3361–3370.
Ganigué, R., Naert, P., Candry, P., de Smedt, J., Stevens, C.V. & Rabaey, K. (2019) Fruity flavors from waste: a novel process to upgrade crude glycerol to ethyl valerate. *Bioresource Technology*, 289, 121574.
Garcia-Garcia, G., Fernandez, M.C., Armstrong, K., Woolass, S. & Styring, P. (2021) Analytical review of life-cycle environmental impacts of carbon capture and utilization technologies. *ChemSusChem*, 14, 995–1015.
Ge, S., Usack, J.G., Spirito, C.M. & Angenent, L.T. (2015) Long-term n-Caproic acid production from yeast-fermentation beer in an anaerobic bioreactor with continuous product extraction. *Environmental Science and Technology*, 49, 8012–8021.
González-Cabaleiro, R., Lema, J.M. & Rodríguez, J. (2015) Metabolic energy-based modelling explains product yielding in anaerobic mixed culture fermentations. *PLoS One*, 10, e0126739.
González-Cabaleiro, R., Lema, J.M., Rodríguez, J. & Kleerebezem, R. (2013) Linking thermodynamics and kinetics to assess pathway reversibility in anaerobic bioprocesses. *Energy & Environmental Science*, 6, 3780–3789.
Groher, A. & Weuster-Botz, D. (2016a) Comparative reaction engineering analysis of different acetogenic bacteria for gas fermentation. *Journal of Biotechnology*, 228, 82–94.
Groher, A. & Weuster-Botz, D. (2016b) General medium for the autotrophic cultivation of acetogens. *Bioprocess and Biosystems Engineering*, 39, 1645–1650.
Huang, S., Kleerebezem, R., Rabaey, K. & Ganigué, R. (2020) Open microbiome dominated by *Clostridium* and *Eubacterium* converts methanol into i-butyrate and n-butyrate. *Applied Microbiology and Biotechnology*, 104, 5119–5131.
Jonczyk, P., Takenberg, M., Hartwig, S., Beutel, S., Berger, R.G. & Scheper, T. (2013) Cultivation of shear stress sensitive microorganisms in disposable bag reactor systems. *Journal of Biotechnology*, 167, 370–376.
Kim, H., Jeon, B.S. & Sang, B.-I. (2019) An efficient new process for the selective production of odd-chain carboxylic acids by simple carbon elongation using Megasphaera hexanoica. *Scientific Reports*, 9, 11999.
Kleerebezem, R. & Stams, A.J.M. (2000) Kinetics of syntrophic cultures: a theoretical treatise on butyrate fermentation. *Biotechnology and Bioengineering*, 67, 529–543.
Kleerebezem, R. & Van Loosdrecht, M.C.M. (2010) A generalized method for thermodynamic state analysis of environmental systems. *Critical Reviews in Environmental Science and Technology*, 40, 1–54.
Koytsoumpa, E.I., Bergins, C. & Kakaras, E. (2018) The CO_2 economy: review of CO_2 capture and reuse technologies. *The Journal of Supercritical Fluids*, 132, 3–16.
Kremp, F. & Müller, V. (2020) Methanol and methyl group conversion in acetogenic bacteria: biochemistry, physiology and application. *FEMS Microbiology Reviews*, 45, fuaa040.
Lang, K., Zierow, J., Buehler, K. & Schmid, A. (2014) Metabolic engineering of pseudomonas sp. strain VLB120 as platform biocatalyst for the production of isobutyric acid and other secondary metabolites. *Microbial Cell Factories*, 13, 2.
Li, F., Hinderberger, J., Seedorf, H., Zhang, J., Buckel, W. & Thauer, R.K. (2008) Coupled ferredoxin and Crotonyl coenzyme a (CoA) reduction with NADH catalyzed by the Butyryl-CoA dehydrogenase/Etf complex from *Clostridium kluyveri*. *Journal of Bacteriology*, 190, 843–850.
Liew, F.M., Martin, M.E., Tappel, R.C., Heijstra, B.D., Mihalcea, C. & Köpke, M. (2016) Gas fermentation-a flexible platform for commercial scale production of low-carbon-fuels and chemicals from waste and renewable feedstocks. *Frontiers in Microbiology*, 7, 694.
Litty, D. & Müller, V. (2021) Butyrate production in the acetogen *Eubacterium limosum* is dependent on the carbon and energy source. *Microbial Biotechnology*, 14, 1–7.
Liu, B., Popp, D., Müller, N., Sträuber, H., Harms, H. & Kleinsteuber, S. (2020) Three novel clostridia isolates produce n-Caproate and iso-butyrate from lactate: comparative genomics of chain-elongating bacteria. *Microorganisms*, 8, 1970.
Lynd, L.H. & Zeikus, J.G. (1983) Metabolism of H_2-CO_2, methanol, and glucose by Butyribacterium methylotrophicum. *Journal of Bacteriology*, 153, 1415–1423.
Mariën, Q., Candry, P., Hendriks, E., Carvajal-Arroyo, J.M. & Ganigué, R. (2022) Substrate loading and nutrient composition steer caproic acid production and biofilm aggregation in high-rate granular reactors. *Journal of Environmental Chemical Engineering*, 10, 107727.
Martens, J.A., Bogaerts, A., Kimpe, N.D. & Jacobs, P.A. (2017) The chemical route to a carbon dioxide neutral world. *ChemSusChem*, 10, 1039–1055.
Martin, M.E., Richter, H., Saha, S. & Angenent, L.T. (2016) Traits of selected *Clostridium* strains for syngas fermentation to ethanol: syngas fermentation strain comparison. *Biotechnology and Bioengineering*, 113, 531–539.
Moscoviz, R., Trably, E., Bernet, N. & Carrère, H. (2018) The environmental biorefinery: state-of-the-art on the production of hydrogen and value-added biomolecules in mixed-culture fermentation. *Green Chemistry*, 20, 3159–3179.
Pacaud, S., Loubière, P., Goma, G. & Lindley, N.D. (1986) Organic acid production during methylotrophic growth of *Eubacterium limosum* B2: displacement towards increased butyric acid yields by supplementing with acetate. *Applied Microbiology and Biotechnology*, 23, 330–335.
Petrognani, C., Boon, N. & Ganigué, R. (2020) Production of isobutyric acid from methanol by *Clostridium luticellarii*. *Green Chemistry*, 22, 8389–8402.
Ritchie, H. (2020) *Sector by sector: where do global greenhouse gas emissions come from?*. Our World in Data. https://ourworldindata.org/ghg-emissions-by-sector [Accessed 22 April 2022].
Ramió-Pujol, S., Ganigué, R., Bañeras, L. & Colprim, J. (2015) Incubation at 25°C prevents acid crash and enhances alcohol production in *Clostridium carboxidivorans* P7. *Bioresource Technology*, 192, 296–303.
Richter, H., Molitor, B., Wei, H., Chen, W., Aristilde, L. & Angenent, L.T. (2016) Ethanol production in syngas-fermenting *Clostridium ljungdahlii* is controlled by thermodynamics rather than by enzyme expression. *Energy & Environmental Science*, 9, 2392–2399.
Schuchmann, K. & Müller, V. (2014) Autotrophy at the thermodynamic limit of life: a model for energy conservation in acetogenic bacteria. *Nature Reviews Microbiology*, 12, 809–821.
Seedorf, H., Fricke, W.F., Veith, B., Brüggemann, H., Liesegang, H., Strittmatter, A. et al. (2008) The genome of *Clostridium kluyveri*, a strict anaerobe with unique metabolic features. *Proceedings of the National Academy of Sciences of the United States of America*, 105, 2128–2133.
Song, C. (2006) Global challenges and strategies for control, conversion and utilization of CO_2 for sustainable development involving energy, catalysis, adsorption and chemical processing. *Catalysis Today*, 115, 2–32.

Stams, A.J.M. (1994) Metabolic interactions between anaerobic bacteria in methanogenic environments. *Antonie Van Leeuwenhoek*, 66, 271–294.

Tomé, D. (2021) Yeast extracts: nutritional and flavoring food ingredients. *ACS Food Science and Technology*, 1, 487–494.

Vees, C.A., Neuendorf, C.S. & Pflügl, S. (2020) Towards continuous industrial bioprocessing with solventogenic and acetogenic clostridia: challenges, progress and perspectives. *Journal of Industrial Microbiology & Biotechnology*, 47, 753–787.

Wang, Q., Wang, C.-D., Li, C.-H., Li, J.-G., Chen, Q. & Li, Y.-Z. (2015) *Clostridium luticellarii* sp. nov., isolated from a mud cellar used for producing strong aromatic liquors. *International Journal of Systematic and Evolutionary Microbiology*, 65, 4730–4733.

Worden, R.M., Grethlein, A.J., Jain, M.K. & Datta, R. (1991) Production of butanol and ethanol from synthesis gas via fermentation. *Fuel*, 70, 615–619.

Zhang, K., Woodruff, A.P., Xiong, M., Zhou, J. & Dhande, Y.K. (2011) A synthetic metabolic pathway for production of the platform chemical Isobutyric acid. *ChemSusChem*, 4, 1068–1070.

SUPPORTING INFORMATION

Additional supporting information can be found online in the Supporting Information section at the end of this article.

How to cite this article: Mariën, Q., Regueira, A. & Ganigué, R. (2023) Steerable isobutyric and butyric acid production from CO_2 and H_2 by *Clostridium luticellarii*. *Microbial Biotechnology*, 00, 1–16. Available from: https://doi.org/10.1111/1751-7915.14321